# Thermo and pH Dual-Controlled Charge Reversal Amphiphilic Graft Copolymer Micelles for Overcoming Drug Resistance in Cancer Cells

**Haitao Zhang [a], Xiao-dong Fan [a, *], Fei Li [b], Rongtian Suo [a], Hui Li [a], Zhen Yang [a], Wanbin Zhang [a], Yang Bai [c], Wei Tian [a, *]**

[a] The Key Laboratory of Space Applied Physics and Chemistry, Ministry of Education and Shaanxi Key Laboratory of Macromolecular Science and Technology, School of Science, Northwestern Polytechnical University, Xi'an, 710072, P. R. China

[b] Department of Pharmacy, 456 Hospital of People's Liberation Army, Ji'nan 250000, China

[c] Xi'an Modern chemistry Research Institute, Xi'an, 710065, P. R. China

## 1 Synthesis of hydroxyl -poly(*N*, *N*-dimethylaminoethyl methacrylate) (HO-PDMA$_{2.1k}$)

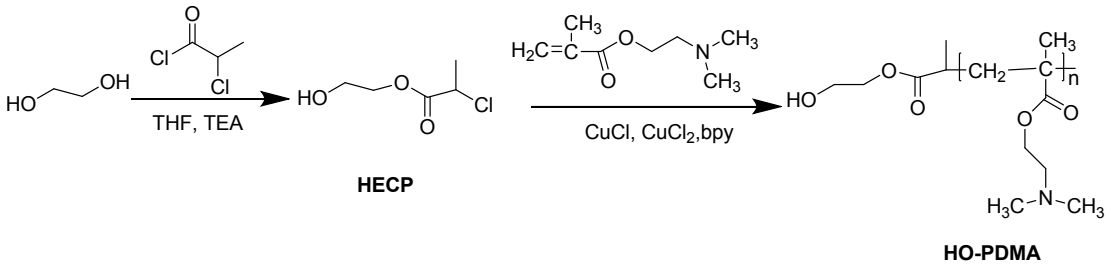


**Scheme S1** Synthesis of HO-PDMA

### 1.1 Synthesis of 2-hydroxyethyl-2-chloropropanoate (HECP).

ATRP initiator **HECP** was synthesized according to prior report with some change.[1] 2-Chloropropionyl chloride was reacted with cold anhydrous ethylene glycol (excess) under stirring for 4 h. The molar ratio of ethylene glycol and 2-chloropropionyl chloride was 20 in order to avoid coupling reaction. The reaction mixture was added to deionized water, and the product attained was extracted by methylene chloride. The organic solution was washed with water and dried over anhydrous magnesium sulfate. The final product was isolated as a colorless liquid upon removal of the solvent， and it was dried under vacuum at r.t. for 24 hours. Yield: 92.3%. $^1$H NMR ($CDCl_3$, 298 K): 1.72 (d, $CH_3$), 1.93 (t, OH), 3.88 (q,-CH(Cl)-COO-), 4.32 (t,-COO-$CH_2$–), 4.45 (q,-O-$CH_2$-).

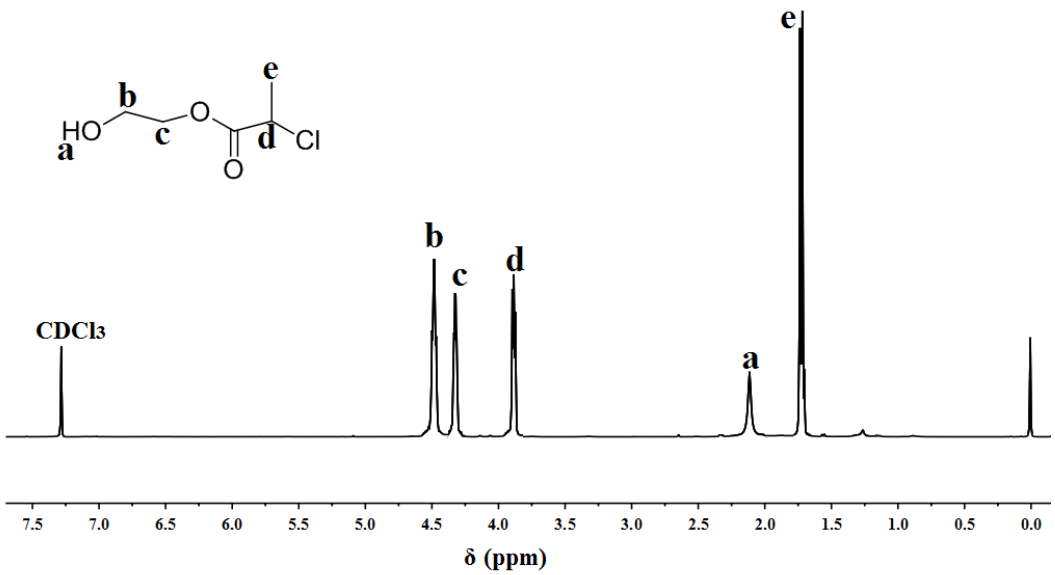


Figure S1 $^{1}$H NMR spectra of HECP in $CDCl_3$

**1.2 Synthesis of hydroxyl -poly(*N*, *N*-dimethylaminoethyl methacrylate) (HO-PDMA$_{2.1k}$)**

A clean and dry Schlenk flask was charged with DMA (0.227g, 1.766 mmol), bpy (0.551g, 3.532 mmol), methanol (4.0 mL) and 2-butanone (6 mL). After one freeze-thaw cycle, CuCl (13.10 mg, 0.132 mmol) and $CuCl_2$ (4.4 mg, 0.033 mmol) were quickly added to the frozen mixture under the protection of $N_2$. The reaction tube was carefully degassed by three freeze-pump-thaw cycles, sealed under a vacuum, and the mixture was then stirred at 20 $^{o}$C .The reaction was stopped after 1 h, via exposure to air and dilution with methanol. The solution was filtered through a column filled with neutral alumina to remove the copper complex before the polymer was precipitated twice in cold THF and dried under vacuum at r.t. for two days. Yield: 46.7%. The structure and molecular weight of the copolymer were determined by $^{1}$H NMR and SEC-MALLS. $^{1}$H NMR (400 MHz,$D_2O$): 4.15 (m O-$CH_2$), 2.59 (br, N-$CH_2$), 2.23 (m N-$CH_3$), 1.75 (s -$CH_2$-), 0.96 (C-$CH_3$). GPC (DMF as eluent): $M_w$ = 2100, $M_w/M_n$

= 1.24.

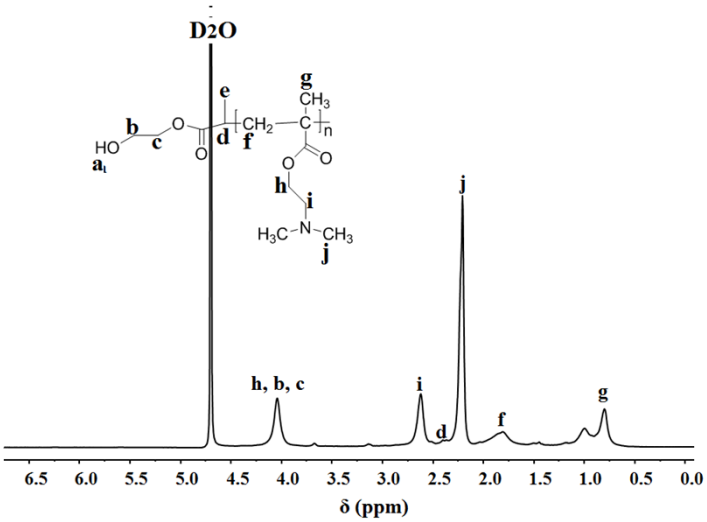


**Fig. S2** $^{1}H$ NMR spectra of HO-PDMA in$D_2O$

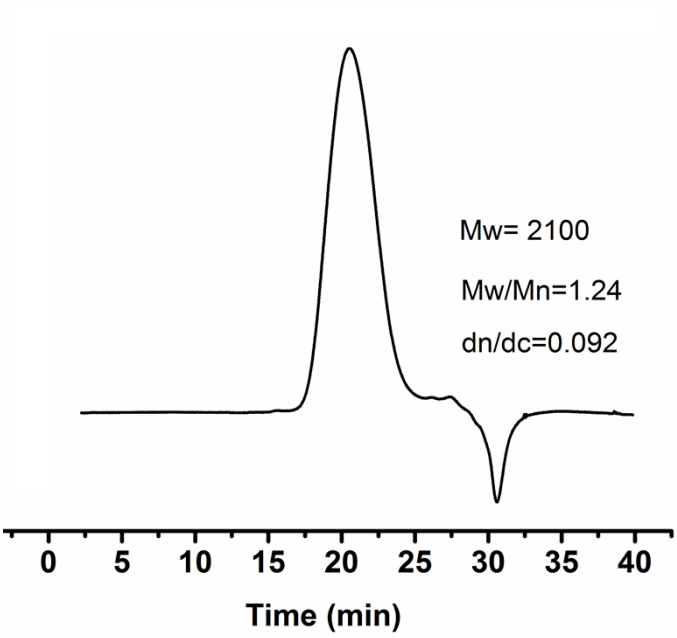


**Fig. S3** DRI signals of SEC/MALLS chromatograms of HO-PDMA (0.5mg $mL^{-1}$).

## 2. Thermo-and pH-sensitivity of $PSMA_{89}$-*g*-$P(DMA_{16}$-*co*-$SD_{56})$ micelles

TEM and DLS were used to further prove the thermo and pH responsive property. Figure S4 shows the TEM images of typical micelles self-assembled from $PSMA_{89}$-*g*-$P(DMA_{16}$-*co*-$SD_{56})$ at temperatures below and above the LCST at pH 7.4

and pH 6.8. It was found that the $D_{av}$ $PSMA_{89}$-*g*-$P(DMA_{16}$-*co*-$SD_{56})$ micelles was 171 nm with a core-shell morphology at pH 7.4 and 37 ºC(Figure S4 A).This result coincident with the TEM result at 25 ºC and pH7.4 (Figure3B-d). Therefore, $PSMA_{89}$-*g*-$P(DMA_{16}$-*co*-$SD_{56})$ micelles could have a stable morphology in physiological environments. The $D_{av}$ of $PSMA_{89}$-*g*-$P(DMA_{16}$-*co*-$SD_{56})$ micelles decreased to 89 nm when temperature increases above the LCST (e.g., 42 ºC) (Figure S4 B). That because the micelles shell containing PDMA blocks shrank, and then the micelles compacted and the size decrease.[2] However, as shown in figure S4 C, when the pH was adjusted to 6.8 at 42 ºC, we got a core-shell nanoparticle with a $D_{av}$ of 162 nm again. The reason is that PDMA becomes a typical cationic polyelectrolyte and is water-soluble at pH 6.8.[3] This change on $PSMA_{89}$-*g*-$P(DMA_{16}$-*co*-$SD_{56})$ micelles can be further identified by DLS (Figure S4 D). Thus, as a drug delivery, $PSMA_{89}$-*g*-$P(DMA_{16}$-*co*-$SD_{56})$ micelles could inhibit the drug burst release in normal physiological environment.

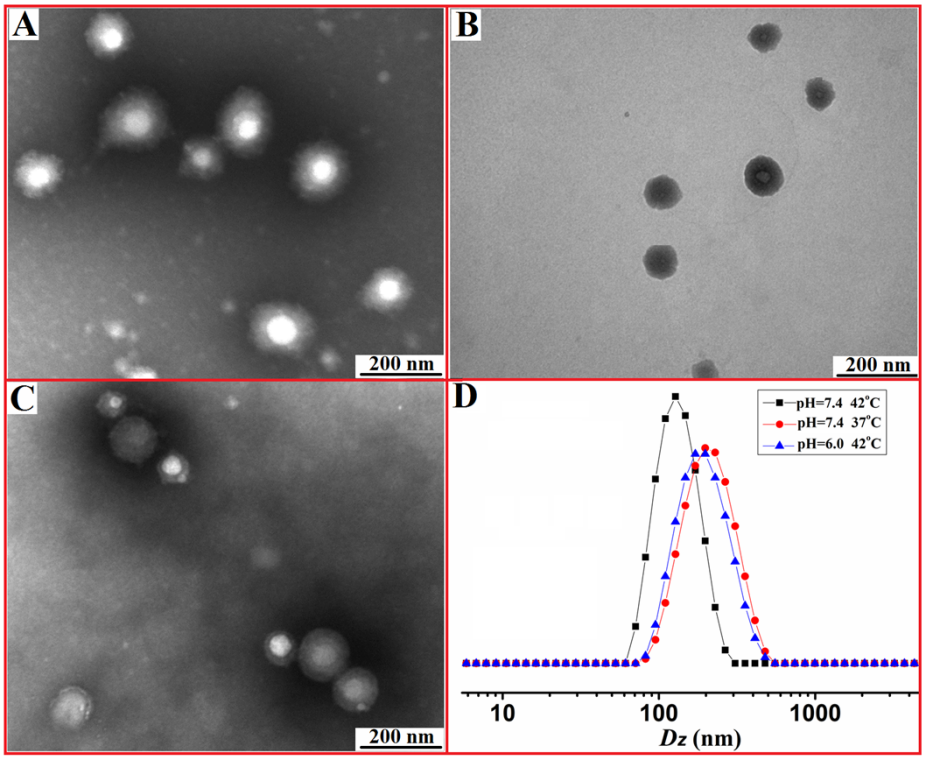


Figure S4 TEM image PSMA$_{89}$-*g*-P(DMA$_{16}$-*co*-SD$_{56}$) micelles at pH 7.4(A) without stain and pH 6.8 (B) stained with 2% phosphotungstic acid ,at 42°C， Size distribution of PSMA$_{89}$-*g*-P(DMA$_{16}$-*co*-SD$_{56}$) nanoparticles in distilled water (0.1 mg/mL) at pH 7.4, 25ºC and pH7.4, 37and 42 ºC

**3. Ztea potential change of PSMA$_{89}$-g-P(DMA$_{16}$-co-SD$_{13}$) micelles and PSMA$_{89}$-g-P(DMA$_{16}$-co-SD$_{31}$) micelles.**

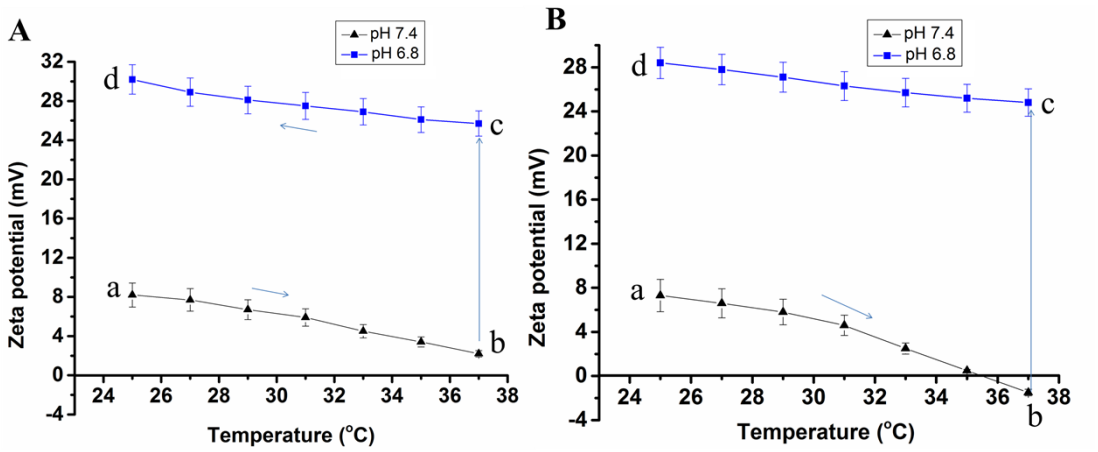

**Figure S5** Zeta potential value of $PSMA_{89}$-g-P($DMA_{16}$-co-$SD_{13}$) micelles (A) and $PSMA_{89}$-g-P($DMA_{16}$-co-$SD_{31}$) (B) micelles as a function of solution temperature. (a-b) temperature increased from 25 °C to 37 °C at pH 7.4; (b-c) pH was adjusted from 7.4 to 6.8 at 37 °C; (c-d) temperature decreased to 25 °C at pH 6.8.

As shown in Figure S5, The zeta potential of $PSMA_{89}$-g-P($DMA_{16}$-co-$SD_{13}$) micelles and $PSMA_{89}$-g-P($DMA_{16}$-co-$SD_{31}$) micelles decreased with the increase with temperature at pH 7.4, and the zeta potential were increased sharply after pH was adjusted to 6.8, which were all similar with the $PSMA_{89}$-g-P($DMA_{16}$-co-$SD_{56}$) micelles, In addition, the zeta potential of $PSMA_{89}$-g-P($DMA_{16}$-co-$SD_{31}$) was positive charged while the zeta potential of $PSMA_{89}$-g-P($DMA_{16}$-co-$SD_{31}$) was negative charged after temperature increased to 37 $^{o}$C at pH 7.4. This indicated that the count SD had great influence on the zeta potential. Moreover, although the LCST of $PSMA_{89}$-g-P($DMA_{16}$-co-$SD_{13}$) micelles and $PSMA_{89}$-g-P($DMA_{16}$-co-$SD_{31}$) micelles were all lower than 37 $^{o}$C (Figure 3A), but their zeta potential shown no sharply change above their LCST. This result indicated that the thermo-sensitivity of the micelles had no effect on the change of zeta potential.

## 4. pKa of $PSMA_{89}$-g-P($DMA_{16}$-co-$SD_{56}$)

In order to understand the influence of temperature on the ionization behavior of $PSMA_{89}$-g-P($DMA_{16}$-co-$SD_{56}$) and calculate their pKa values, a stepwise titration of polymer solution with NaOH was conducted at different temperature. As shown in Figure S6A，the titration curves for $PSMA_{89}$-g-P($DMA_{16}$-co-$SD_{56}$) at different

temperature were different in shape and $PSMA_{89}$-g-P($DMA_{16}$-co-$SD_{56}$)'s titration curves possessed two plateau regions. Thus $PSMA_{89}$-g-P($DMA_{16}$-co-$SD_{56}$) had two pKa values and temperature had great influence on the $PSMA_{89}$-g-P($DMA_{16}$-co-$SD_{56}$)'s pKa. As shown in Figure S6B, the values for pKa1 and pKa2 of $PSMA_{89}$-g-P($DMA_{16}$-co-$SD_{56}$) decreased from 4.65 to 4.37 and from 6.41 to 5.89, respectively, after the temperature was increased from 25 to 40 $^{o}$C. In addition, at 25 $^{o}$C, the value of pKa1 was similar the pKa of acetic acid (4.75)[4] while the value of pKa2 was similar the pKa of SD (6.25).[5] Therefore the two pKa of PSMA89-g-P(DMA16-co-SD56) may be induced by the existence of SD and –COOH.

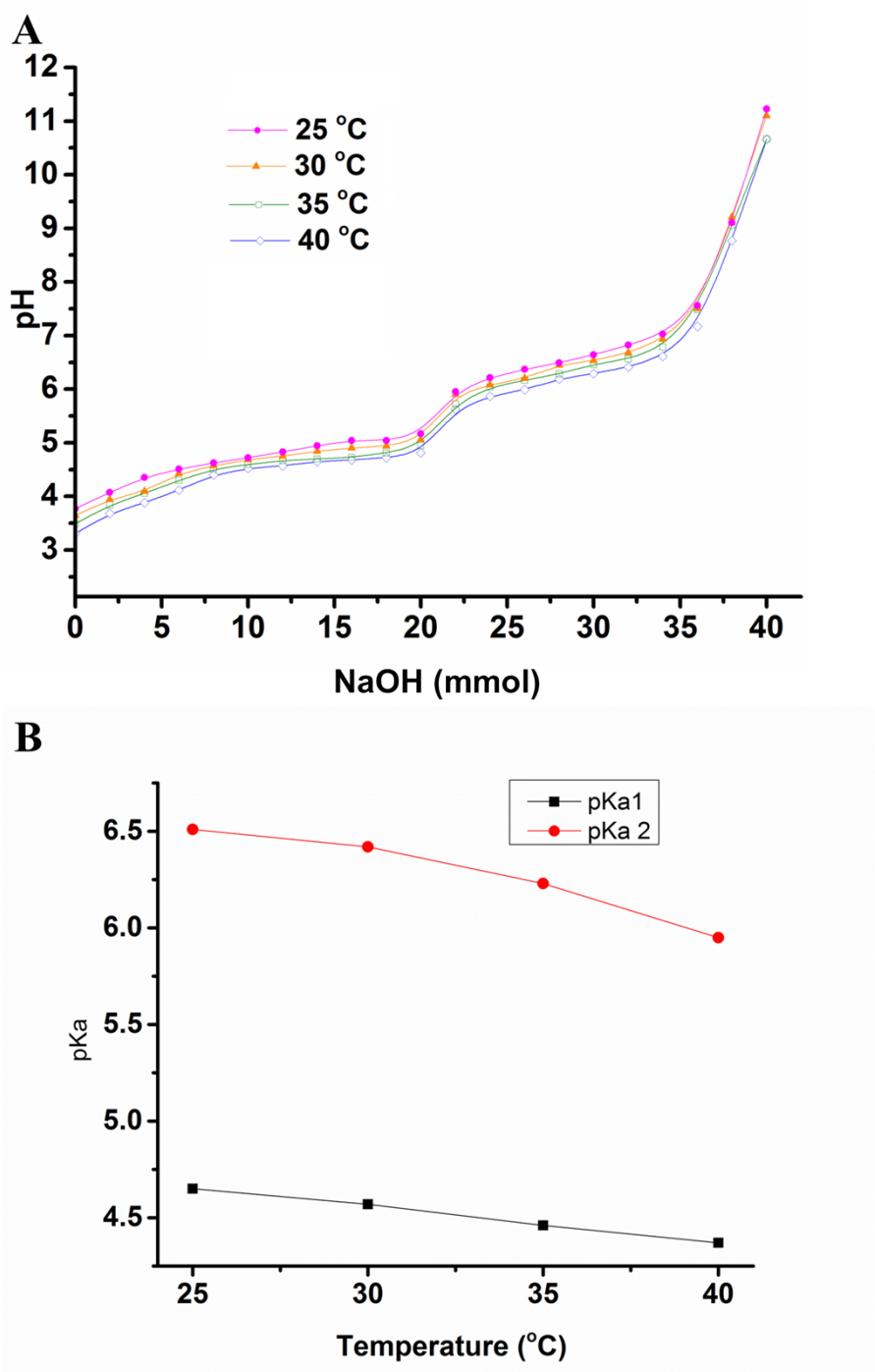


**Figure S6** A: Titration curves (0.1 N NaOH) of $PSMA_{89}$-g-P($DMA_{16}$-co-$SD_{56}$) at different temperature. B: Temperature versus chromatographically determined pKa1 and pKa2. The results are expressed as means ± standard deviations for n=3.

## 5. Dz of DOX loaded $PSMA_{89}$-g-$P(DMA_{16}$-co-$SD_{56})$ micelles and $PSMA_{89}$-g-$P(DMA_{16}$-co-$SD_{56})$ micelles

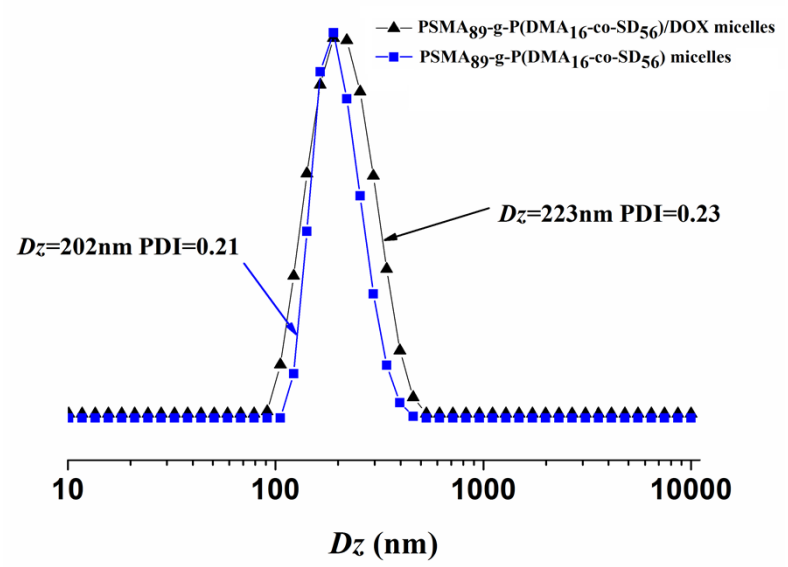


**Figure S7** Typical intensity-averaged diameter distributions of DOX loaded $PSMA_{89}$-g-$P(DMA_{16}$-co-$SD_{56})$ and $PSMA_{89}$-g-$P(DMA_{16}$-co-$SD_{56})$ aqueous solutions at 0.5 mg/mL and 25°C pH 7.4

## 6. LCST and ztea potential change of DOX loaded $PSMA_{89}$-g-$P(DMA_{16}$-co-$SD_{56})$ micelles

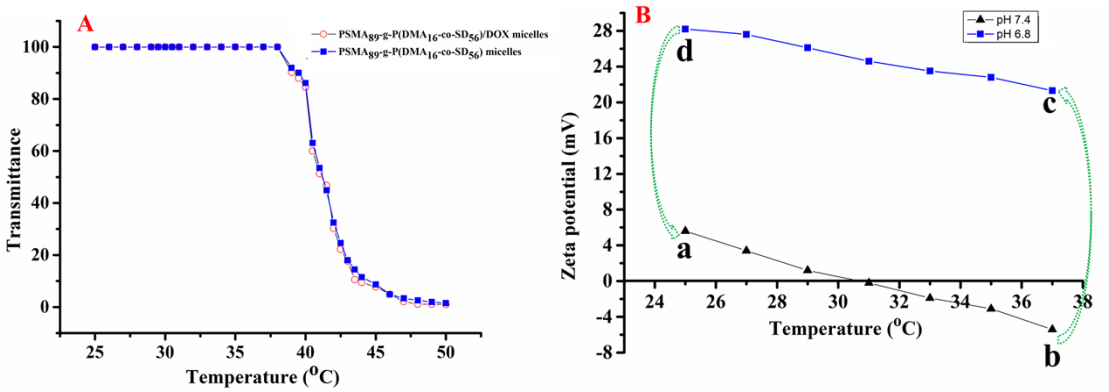


**Figure S8** A: Optical transmittance of DOX loaded $PSMA_{89}$-g-$P(DMA_{16}$-co-$SD_{56})$ micelles and $PSMA_{89}$-g-$P(DMA_{16}$-co-$SD_{56})$ micelles with a concentration of 0.5 mg/mL in phosphate-buffer saline (PBS, pH 7.4); B ztea potential change of DOX loaded $PSMA_{89}$-g-$P(DMA_{16}$-co-$SD_{56})$ micelles with temperature

Table S1 LCST and Zeta potential of $PSMA_{89}$-g-P($DMA_{16}$-co-$SD_{56}$) micelles at pH 7.4

| Concentration (mg/ml) | LCST ($^oC$) | Zeta potential (mV) 25 $^oC$ | 37$^oC$ |
|---|---|---|---|
| 0.5 | 38.3 | 4.3 | -6.1 |
| 1 | 38.1 | 4.5 | -6.3 |
| 1.5 | 38.0 | 4.4 | -6.2 |

## 7. Reference


1. Z. Yin, C. Koulic, C. Pagnoulle, and R. JérÔme. *Macromolecules,* 2001**, 34***,* 5132-5139

2. W. Z. Yuan, H. Zou, W. Guo, A. Wang, and J. Ren. *J. Mater. Chem.*, 2012, **22**, 24783–24791.

3. X. Han, X. X. Zhang, H.F. Zhu, Q. Y. Yin, H. L. Liu, and Y. Hu, *Langmuir*, 2013, **29**, 1024−1034

4. K.F. Tjipangandjara, P. Somasundaran, *Adv. Powder Technol.* 1992, **3,** 119-127

5. S. I. Kang and Y. H. Bae, *J. Controlled Release,* 2002, **80**, 145-155.